A Computational Study of Metal–Dinitrogen Co-ordination†

Robert J. Deeth* and Christian N. Field
Inorganic Computational Chemistry Group, School of Chemistry, University of Bath, Claverton Down, Bath BA2 7AY, UK

Local density functional theory (DFT) discrete variational Xα (DVXα) calculations have been performed on the model metal–dinitrogen system *trans*-$[MA_4(N_2)_2]$ (M = Mo, A = PH_3 or SH_2; M = W, A = PH_3) and *trans*-$[MClA_4(N_2)]$ (M = Mo, A = PH_3 or SH_2). Molecular-orbital and charge density analyses demonstrate a reasonable qualitative correlation between theory and experiment with respect to metal–ligand bonding, N–N stretching frequencies, and the sites and relative rates of attack on co-ordinated N_2 by protons and organic radicals. Comparisons with *ab initio* Hartree–Fock theory results for $[Mo(PH_3)(N_2)_2]$ show that the DVXα method gives a better description of the charge distribution. Attempts to quantify the theoretical predictions *via* binding-energy calculations have been less successful. Evidently, a more sophisticated DFT treatment will be required for improved quantitative accuracy.

The interest in metal–dinitrogen co-ordination stems largely from its presumed relevance to biological nitrogen fixation.[1] The active sites of the natural nitrogen-fixing enzymes (nitrogenases) have long been known to contain a Mo/Fe/S co-factor species (FeMo co-factor) which is responsible for binding N_2 and for mediating its subsequent protonation and reduction to ammonia.[2] The molybdenum site of the enzyme co-factor was believed to bind the incoming ligand and this result stimulated extensive studies of model Mo–N_2 chemistry. Dinitrogen also binds to a variety of other metals which is significant since other nitrogenase N_2-reducing co-factors have emerged which contain vanadium or iron instead of molybdenum.

Extensive synthetic studies of model complexes have demonstrated the co-ordination of the ligand to several metals in several different modes.[3] In mononuclear complexes there is a preference for end-on binding analogous to the case for the isoelectronic CO ligand. These species display varying degrees of the catalytic activity of FeMo co-factor although often the isolated species contains phosphorus ligands which are not biologically relevant.

The general features of end-on M–N_2 are reasonably well understood.[4] Qualitatively, strong M–N_2 interactions are obtained for metals towards the left of the transition series centred on the Cr/Mo/W triad. Stability also increases on descending a given periodic group. The bonding is described by the basic σ-bonding/π-back bonding picture familiar in the isoelectronic carbonyl ligand although N_2 is generally considered to be both a weaker σ donor and a poorer π acceptor than CO. In common with carbonyl chemistry, the infrared stretching frequency ν(N–N) is associated with a decreasing bond order, greater π back donation and hence a stronger M–N bond.

However, the recent crystallographic studies on nitrogenase[5] itself pose many new questions. The structural data suggest that molybdenum may not be the site of N_2 co-ordination after all and this opens up the possibility that end-on co-ordination may not be the most favourable binding mode. Deng and Hoffmann[6] have recently investigated these issues *via* extended-Hückel molecular orbital (EHMO) calculations of N_2 binding to a FeMo co-factor model system derived from the latest structural data. They favour a side-on bridging position between two Fe atoms shown in structure **I** (Fig. 1) although the two end-on bridging structures **II** and **III** are also possibilities.

However, the EHMO method is a relatively limited theoretical procedure for probing the bonding and charge distributions in transition-metal systems. A more sophisticated method is required for a better understanding of the factors

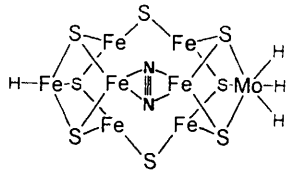

I

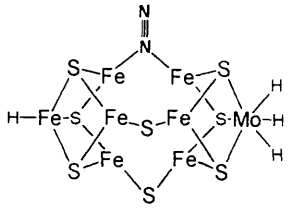

II

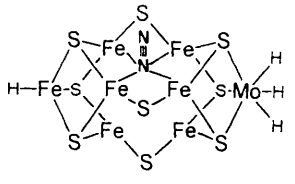

III

Fig. 1 Proposed N_2 co-ordination modes and sites for model FeMo co-factor system[6]

† *Supplementary data available* (No. SUP 57010, 11 pp.): molecular orbital energies and percentage atomic orbital contributions. See Instructions for Authors, *J. Chem. Soc., Dalton Trans.*, 1994, Issue 1, pp. xxiii–xxviii.

Non-SI units employed: $E_h \approx 4.36 \times 10^{-18}$ J, eV $\approx 1.60 \times 10^{-19}$ J.

controlling dinitrogen binding and reactivity. We believe that schemes based on density functional theory (DFT)[7] serve the purpose well. The initial aim of these studies is to investigate how well DFT-based methods can account for some known experimental facts. In particular, while much of the co-ordination chemistry of dinitrogen has involved phosphines as co-ligands, sulfur-based species are more biologically relevant and complexes employing saturated sulfur macrocycles appear to activate bound dinitrogen more than their phosphine analogues.[8]

Calculations are reported for simple model Mo–N_2 complexes with PH_3 and SH_2 as co-ligands. The tungsten compound, $[W(PH_3)_4(N_2)_2]$, and, for comparison, the relevant isolated ligands are included also. The particular scheme used is the discrete variational Xα (DVXα) method[9] which has been shown[10] to give good descriptions of the static electronic structures and bonding in a variety of metal complexes. We seek here to establish how well the chemistry of known dinitrogen complexes is described. Subsequent papers will examine other molecules, both with different metals and more complex ligand systems, and will explore extensions of and enhancements to the DVXα scheme itself.

Computational Details

The molecules examined here are *trans*-$[MoA_4(N_2)L]$ (A = PH_3 or SH_2, L = N_2 or Cl) and *trans*-$[W(PH_3)_4(N_2)_2]$ plus, for comparison, the isolated ligands PH_3, SH_2 and N_2. A full description of the DVXα method used here has been given before.[10a] Optimised minimal single-site orbital (SSO) atomic basis sets[11] were employed for all atoms except the transition metals where an additional 5p orbital on Mo or 6p orbital on W was added. DVXα SSO basis functions are roughly equivalent to a double-ζ quality expansion. All calculations are spin restricted and non-relativistic and employ the self consistent charge (SCC) procedure[12] which computes the Coulomb potential relative to overlapping (spherical) atomic electron densities derived from a Mulliken population analysis.[13] Frozen cores[14] are employed throughout: up to 2p for Cl, P and S; up to 4p for Mo and up to 5p for W.

Bond lengths for the bis(dinitrogen) complexes were derived from X-ray crystal structure analyses of *trans*-$[Mo(dppe)_2(N_2)_2]$[15] (dppe = $Ph_2PCH_2CH_2PPh_2$), *trans*-$[W(PPhEt_2)_4(N_2)_2]$[16] and $[Mo(N_2)_2L]$[8a] (L = 3,3,7,7,11,11,15,15-octamethyl-1,5,9,13-tetrathiacyclohexadecane). The latter has a macrocyclic ring in the 'all-up' conformation such that the plane of four S atoms sits above the rest of the macrocycle. This molecule has approximately C_{4v} symmetry which has therefore been imposed on all the molecules studied here. The geometries have been further idealised such that the M–N–N angles are 180° and that the metal lies in the equatorial plane. All angles at the metal are therefore 90°. The Mo–Cl bond length in $[MoClA_4(N_2)]$, L = PH_3 or SH_2 was chosen as 2.416 Å[17] with the rest of the molecule remaining unchanged. The H–P–H and H–S–H angles were fixed at 107 and 105° respectively with the bond lengths to H fixed at the free-ligand values. The geometrical data and the number of DVXα sample points used for each molecule are collected in Table 1 while relevant vibrational data are given in Table 2. The number and distribution of sample points ensures a numerical error of approximately 0.02 eV in MO energies and 0.002 in orbital populations.

Binding energies were computed *via* the algorithm developed by Delley *et al.*[20] The binding energy for the molecule is calculated by subtracting from the total molecular energy the contributions from the isolated atoms. The sample point grid for the atoms is matched exactly with that for the molecule. This provides greater accuracy since errors in numerical sampling, which can lead to large energy fluctuations near nuclei, are cancelled out. In order to estimate the M–N_2 bond energy, separate binding energies for the ML_4 (L = PH_3 or SH_2) and N_2 moieties were computed and subtracted from the total for the relevant whole molecule. The N–N symmetric stretch vibrational energies were estimated by performing three binding-energy calculations for three different N–N distances (keeping the distance between the metal and the midpoint of the N–N bond constant) and fitting the resulting energies to a harmonic function using a reduced mass appropriate to the M–N–N moiety.

Ionisation potentials were computed using Slater's transition-state formalism[21] and all atomic-orbital and overlap populations were computed *via* Mulliken's procedure.[13]

Results and Discussion

The general accuracy of the DVXα SCC method was first gauged by computing the electronic structures of the isolated ligands N_2, PH_3 and SH_2. These molecules have been the subject of many previous studies, including DVXα treatments.[12,22] The present results compare favourably although more sophisticated methods can produce better agreement with experiment.

For N_2, the DVXα SCC ground state MO sequence is the same as that derived from photoelectron spectroscopy data;[23] that is, the occupied levels decrease in the order $2\sigma_g > 1\pi_u > 1\sigma_u > 1\sigma_g$. Transition-state calculations for the two highest occupied MOs give ionisation potentials of 14.7 and 16.1 eV compared to the experimental values of 15.6 and 17.0 eV respectively. The computed ionisation potentials are *ca.* 1 eV too low, but the difference between the two ionisations is the same for both theory and experiment (1.4 eV).

The absolute agreement is somewhat better for PH_3 where the $2a_1$ and 1e ionisation potentials are computed at 10.75 and 13.55 eV compared to experimental values[24] of 10.58 and 13.50 eV respectively. The first ionisation potential for SH_2 is relatively poorly reproduced (calculated for $1b_1$ orbital 11.05, observed[25] 10.48 eV) while the next two ionisation potentials agree much better (calculated for $2a_1$ 13.41, observed[25] 13.25 eV; calculated for $1b_2$ 15.42, observed[25] 15.35 eV). Overall, the DVXα electronic structures of the ligands are reasonably accurate and this despite the absence of d orbitals on either P or S. This might be expected to have serious implications for the treatment of M–L π bonding. However, it has been shown by very accurate DVXα calculations[22a] that the π-acceptor orbitals in phosphines have a larger contribution from the 3p orbitals than the 3d. Thus, the minimal treatment adopted here includes

Table 1 Bond lengths (Å) and number of DVXα numerical sample points

Compound	M–L_{eq}	M–N	N–N	M–Cl	Number of points	Ref.
$[Mo(PH_3)_4(N_2)_2]$	2.458	2.019	1.119	—	11 435	15
$[Mo(SH_2)_4(N_2)_2]$	2.424	1.999	1.107	—	9 976	8(*a*)
$[MoCl(PH_3)_4(N_2)]$	2.458	2.019	1.119	2.416	11 313	17[a]
$[MoCl(SH_2)_4(N_2)]$	2.424	1.999	1.107	2.416	10 005	17[a]
$[W(PH_3)_4(N_2)_2]$	2.458	2.038	1.191	—	11 437	16

[a] Reference for Mo–Cl distance.

Table 2 Observed N–N vibrational bands (cm^{-1})

Compound	ν(N–N)[a]	Ref.
$[Mo(PH_3)_4(N_2)_2]$	1988 (R), 1925 (IR)[b]	18
	1976 (IR)[c]	18
$[Mo(SH_2)_4(N_2)_2]$	1955, 1890 (IR)[d]	8(*a*)
$[MoCl(PH_3)_4(N_2)]$	1966 (IR)[c]	19
$[W(PH_3)_4(N_2)_2]$	1968 (R), 1891 (IR)[b]	18
	1946 (IR)[c]	18

[a] R = Raman (symmetric stretch), IR = infrared (asymmetric stretch). [b] $Et_2PCH_2CH_2PEt_2$ (depe) equatorial ligands. [c] dppe Equatorial ligands. [d] 3,3,7,7,11,11,15,15-Tetramethyl-1,5,9,13-tetrathiacyclohexadecane equatorial ligands, non-centrosymmetric complex.

the most important functions for describing the metal–ligand interaction.

As far as the metal atoms are concerned, previous minimal basis SSO calculations of molybdenum complexes[10d] yielded excellent agreement with experimental d–d and charge-transfer spectra, suggesting that the non-relativistic Xα method can handle even second-row metals adequately. The same might not be expected to be true *a priori* for a third row metal such as tungsten. However, other non-relativistic studies involving heavy third-row metals apparently give reasonable results.[26] In summary, then, calculations on the constituent ligands, together with previous related work argue for a reliable description of the electronic structure and bonding in the present dinitrogen systems.

Electronic Structures.—Discussions of the bonding and reactivity of transition-metal complexes centre around the nature of the valence MOs. The energies of the relevant functions for the molybdenum–dinitrogen complexes and the isolated ligands are shown schematically in Fig. 2. The computed energy levels for $[W(PH_3)_4(N_2)_2]$ are essentially identical to those of the Mo analogue. Full tables of MO energies and their AO compositions for the complete molecules, the isolated ligands and the ML_4 fragments used for the binding energy calculations have been deposited as supplementary material (SUP 57010).

For all the dinitrogen complexes, the highest occupied MO (HOMO) is the 7e MO which comprises *ca.* 65% metal d_{xz}, d_{yz}, about 10% equatorial-ligand and around 25% axial-ligand contributions. Immediately below the 7e orbital is the main in-plane metal-to-equatorial ligand π function, $2b_2$, with about 75% metal d_{xy} character. A similar result was obtained from Hartree–Fock (HF) calculations on, among other species, $[Mo(PH_3)_4(N_2)_2]$.[27] The metal contributions are much higher (77% and 85% respectively) but HF theory is well known to give too ionic a description of M–L bonding[28] which is probably accentuated even more in this case by the use of relatively small STO-3/4G basis sets. Extended-Hückel MO calculations[4] invert the order of the d_{xy} and $d_{xz,yz}$ orbitals. Assuming that both N_2 and PH_3 act as π acceptors, the EHMO model is predicting much greater π acceptance for N_2 than PH_3. This is also reflected in the EHMO results giving a much larger negative charge on N_2 than is calculated by either of the other two more sophisticated approaches (see below).

For $[Mo(PH_3)_4(N_2)_2]$, the main metal–ligand bonding functions are as follows: Mo–P(σ) $3b_1$ and $7a_1$; Mo–P(π) $2b_2$; Mo–N_2(σ) $8a_1$ and $4a_1$; Mo–N_2(π) 7e. (The $7a_1$ and $4a_1$ functions have energies below −8 eV and are not shown in Fig. 2.) The extent of covalency, as monitored by the percentage of the minor component (either metal or ligand based) in these MOs ranges from *ca.* 7% to *ca.* 26%: $3b_1$, 26% metal; $7a_1$, 15% metal; $2b_2$, 24% ligand; $8a_1$, 7% metal; $4a_1$, 15% metal; 7e 26% ligand. Given that there are twice as many Mo–P bonds as Mo–N bonds, these data imply a greater covalent mixing for Mo–N bonding. This is borne out by metal–ligand overlap

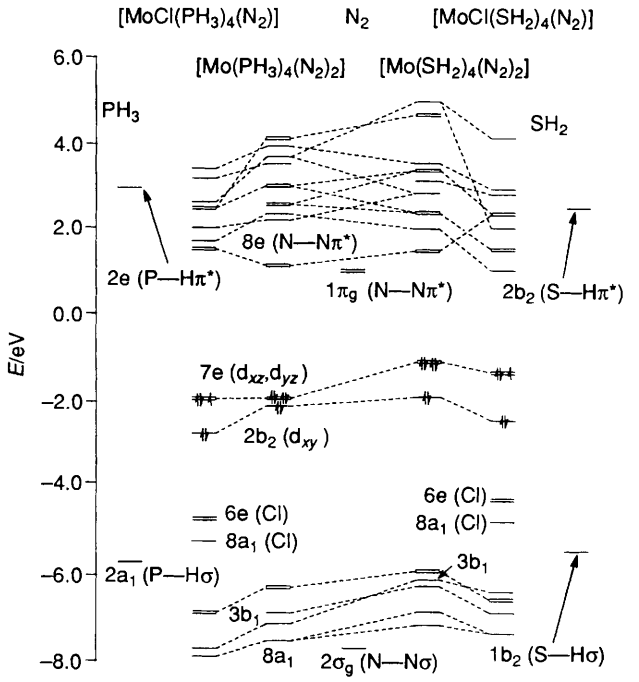

Fig. 2 Molecular orbital energy-level diagram for the model molybdenum–dinitrogen complexes and isolated ligands

populations (Table 3) which are *ca.* 0.5 electron for Mo–P bonds *versus ca.* 0.7 electron for Mo–N_2 overlap.

The nature of the Mo–SH_2 interaction can also be inferred from Fig. 2. There is a general destabilisation of the Mo–S bonding levels (*e.g.* $3b_1$, $2b_2$) indicating a weaker interaction relative to PH_3. The overlap populations are commensurately smaller by *ca.* 0.1 e (Table 3). The most striking change on moving from $[Mo(PH_3)_4(N_2)_2]$ to $[Mo(SH_2)_4(N_2)_2]$ is the larger splitting between the 7e and $2b_2$ MOs. The increase in energy of the $2b_2$ orbital is consistent with a diminished π-acceptor role in the equatorial plane. Perpendicular to this plane are the S lone pairs. Conventional ligand-field arguments would suggest a π-donor role for such lone-pair electrons consistent with the large destabilisation of the 7e orbitals. A sulfur π-donor function has also been suggested on the basis of EHMO calculations on a D_{4h} *trans*-$[Mo(SH_2)_4(N_2)_2]$ model complex.[8a] Evidently, the transition from planar sp^2-type SH_2 ligands in the EHMO study to the bent sp^3-type SH_2 ligands used here does not alter the qualitative features of the π bonding.

Metal–N≡N Bonding in Detail.—A more detailed breakdown of the M–N and N–N overlap populations into separate σ and π contributions is also presented in Table 3. It is of interest to compare these data with the stability of the M–N_2 bond and the variation of the N–N stretching frequencies.

For the bis(dinitrogen) complexes, the DVXα M–N overlap population, and hence M–N_2 stability, increases in the series: $[Mo(PH_3)_4(N_2)_2]$ < $[W(PH_3)_4(N_2)_2]$ < $[Mo(SH_2)_4(N_2)_2]$. This sequence is consistent with experiment in that the tungsten compound is more stable than its Mo analogue while the sulfur species $[Mo(N_2)_2]$[8a] is even more stable, decomposing only above 135 °C.

Comparisons between the observed vibrational stretching frequencies and the computed N–N overlaps are hampered by the dependence of the former on the phosphine substituents. For a given metal, the change from ethyl-substituted depe to phenyl-substituted dppe is accompanied by a *ca.* 50 cm^{-1} increase in the infrared asymmetric-stretch energy as compared to a *ca.* 30 cm^{-1} decrease in ν(N–N) for a tungsten complex relative to its molybdenum analogue if the equatorial ligands are identical (see Table 2). The N–N frequency for the sulfur macrocyclic species is therefore lower than for both the depe

Table 3 Dinitrogen charge and overlap populations for M–N_2 co-ordination

Molecule	N_2 charge	N–N(tot)	M–L_{eq}	M–N	N–N(σ)	M–N(σ)	N–N(π)	M–N(π)
N_2	0.0	1.459	—	—	0.535	—	0.924	—
$[Mo(PH_3)_4(N_2)_2]$	−0.097	1.369	0.472	0.641	0.591	0.441	0.777	0.200
$[Mo(SH_2)_4(N_2)_2]$	−0.154	1.354	0.287	0.672	0.589	0.439	0.765	0.233
$[MoCl(PH_3)_4(N_2)]$[a]	−0.134	1.338	0.443	0.656	0.586	0.434	0.752	0.222
$[MoCl(SH_2)_4(N_2)]$[b]	−0.172	1.361	0.292	0.644	0.607	0.408	0.754	0.236
$[W(PH_3)_4(N_2)_2]$	−0.127	1.280	0.483	0.667	0.588	0.448	0.691	0.219

[a] Mo–Cl overlap = 0.401. [b] Mo–Cl overlap = 0.408.

bis(dinitrogen) complexes but lies in between the frequencies for the dppe analogues.

The latter pattern is, incidentally, predicted theoretically given that a decreasing ν(N–N) for the symmetric or asymmetric stretch is to be associated with a weakening N–N bond and therefore with a smaller overlap population (Table 3). However, one would ideally like to perform calculations on the actual molecules rather than on truncated model systems in order to be more confident about making comparisons between very different molecules.

Nevertheless, it is worth noting that the N–N overlaps do seem to reflect the bonding and are not simply determined by, say, the chosen geometry. Hence, although the lower N–N overlap in $[W(PH_3)_4(N_2)_2]$ may be due in part to the longer N–N bond length employed, the N–N bond length for the Mo–SH_2 complex is shorter than for either $[Mo(PH_3)_4(N_2)_2]$ or $[W(PH_3)_4(N_2)_2]$ yet its N–N overlap lies between those for the former complexes.

A comparison of the vibrational frequencies between $[MoCl(PH_3)_4(N_2)]$ and the other PH_3 molecules is on firmer ground since experimental data are available for a complete series of dppe systems (Table 2). The values of ν(N–N) for the symmetric stretch decrease: $[Mo(dppe)_2(N_2)_2]$ > $[MoCl(dppe)_2(N_2)]$ > $[W(dppe)_2(N_2)_2]$ with values of 1976, 1966 and 1946 cm^{-1} which correlate well with the decreasing N–N overlaps of 1.369, 1.338 and 1.280 respectively.

Protonation of Co-ordinated N_2.—Nitrogen fixation involves the successive protonation and reduction of N_2 to form NH_3. Model systems which can undergo protonation of co-ordinated N_2 are therefore of special importance.

The mechanism of protonation of bis(dinitrogen) complexes is believed to involve initial attack at the terminal end of one of the N_2 ligands.[18,19] It is generally supposed, therefore, that the reaction is charge controlled and that the terminal N (N_{term}) should carry a larger negative charge than the inner-bound N (N_{in}). This has been predicted by electron spectroscopy for chemical applications data[29] and by a variety of calculations including EHMO studies[4] where, for $[Mo(PH_3)_4(N_2)_2]$, charges of −0.67 and +0.05 are predicted for terminal- and inner-bound N atoms respectively. The present DVXα calculations describe a similar story, although the magnitudes of the charges are much smaller (Table 4). The HF treatment of $[Mo(PH_3)_4(N_2)_2]$[27] also gave small charges but in the wrong sense, *i.e.* the inner N was more negative.

On the basis of the gross negative charge on N_2, $[W(PH_3)_4(N_2)_2]$ should be more reactive than the Mo analogue, which agrees with experiment. The N_2 is even more negatively charged in $[Mo(SH_2)_4(N_2)_2]$ and should therefore protonate even more rapidly. This system has been shown to be more reactive than its phosphine counterparts with regard to acylation,[8] but this reaction probably proceeds *via* a different mechanism to protonation. The protonation study has, to our knowledge, not yet been reported.

Acylation/Arylation/Alkylation of Co-ordinated N_2.—Reaction of dinitrogen complexes with organic halides is thought to proceed *via* loss of N_2, attack by RX at the vacant site, cleavage of the R–X bond to give an $[MXA_4(N_2)]$ species which is then attacked at N_2 by the radical generated in the cleavage step.[30] The calculations on the chloro complexes are relevant here in that, given the radical nature of the reaction, the product will be determined by the character of the acceptor orbital on the metal complex, *i.e.* the 7e MO.

Table 4 Atom and ligand gross charges for $[M(PH_3)_4(N_2)_2]$ complexes

Atom/ligand	Mo[a]	W[a]	Mo[b]	Mo[c]
M	−0.064	0.001	−0.59	0.65
N_{in}	0.021	−0.003	0.05	−0.11
N_{term}	−0.118	−0.124	−0.67	−0.03
N_2	−0.097	−0.127	−0.62	−0.14
P	0.045	0.046	—	—
H	0.007	0.006	—	—
PH_3	0.066	0.064	—	−0.09

[a] DVXα method. [b] Extended-Hückel MO method.[4] [c] Hartree–Fock method.[27]

Plots of the 7e MOs for the two chloro complexes $[MoCl(PH_3)_4(N_2)]$ and $[MoCl(SH_2)_4(N_2)]$ are given in Fig. 3. The largest features of these plots are the metal d_π orbitals and the terminal N atom which, given the logarithmic scale, have peak heights four times larger than the features associated with Cl or the equatorial ligands. The terminal N presents the most favourable site of attack, which is consistent with experimental observations. As far as the relative reactivity between the PH_3 and SH_2 systems, the terminal N feature for the SH_2 molecule is marginally larger. However, the difference is quite slight.

Binding-energy Calculations.—The preceding analysis of the electron density in terms of variation in atomic charges and overlap populations correlates quite well with experiment. We therefore decided to try and extend these correlations to a more quantitative calculation of M–N_2 bond energies and N–N stretching frequencies for the bis(dinitrogen) species and N_2. Analytical first and second derivatives are not available in the present DVXα version so these quantities were estimated numerically as described above. The results of these admittedly crude calculations are presented in Table 5.

The theoretical value for ν(N–N) of N_2 is some 600 cm^{-1} too low (observed[3] 2331 cm^{-1}) and already indicates that the DVXα SCC method gives a relatively inaccurate description of the shape of the potential-energy surface at the observed geometries. While the numerical agreement improves dramatically for the Mo complexes where theory is now within about 150 cm^{-1} of experiment, the computed vibrational energy increases from $[Mo(PH_3)_4(N_2)_2]$ to $[Mo(SH_2)_4(N_2)_2]$ while experimentally it decreases. For the tungsten molecule, the computed value is over 500 cm^{-1} lower than the experimental value of the Mo analogue which presumably reflects a relatively poorer treatment of the W–N bond. One is tempted to speculate that relativistic effects which, as described above, do not appear to affect significantly the charge density distribution do influence the total energies. This carries over to the estimated bond energies where E_b for the W–N bond would be expected to be greater than that for the Mo–N link but the DVXα scheme predicts the reverse.

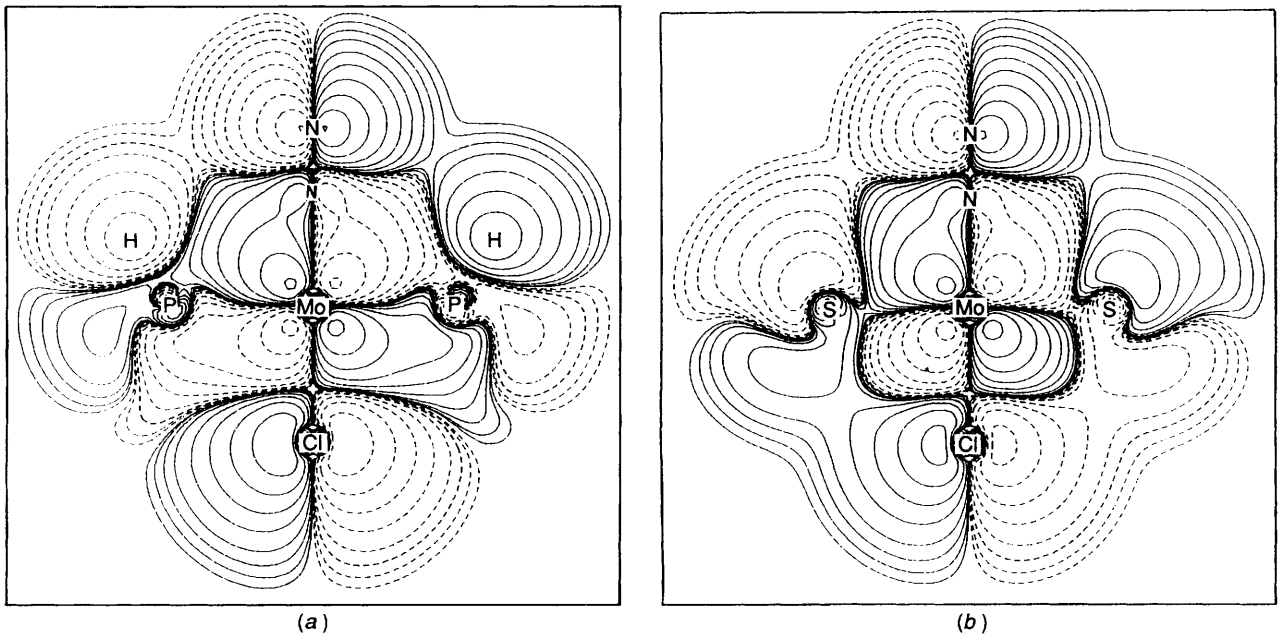

(*a*) (*b*)

Fig. 3 Molecular orbital contour plots of the 7e function of $[MoCl(PH_3)_4(N_2)]$ (*a*) and $[MoCl(SH_2)_4(N_2)]$ (*b*). Solid lines indicate positive contours, dashed lines negative contours. Lowest contours are ± 0.000488 E_h. Successive contour levels differ by a factor of two

Table 5 Computed N–N symmetric stretching frequencies, $\nu_{sym}(cm^{-1})$, and theoretical M–N_2 binding energies, E_b (eV), for bis(dinitrogen) compounds and N_2

Compound	ν_{sym}	E_b
N_2	1765	—
$[Mo(PH_3)_4(N_2)_2]$	1441	7.80
$[Mo(SH_2)_4(N_2)_2]$	1480	7.49
$[W(PH_3)_4(N_2)_2]$	1567	6.92

Evidently, the simple SCC procedure does not produce quantitatively accurate total energies. This is not wholly unexpected since the SCC potential is just an average of overlapping spheres. In addition, it is impractical with the code available to locate the true minimum energy although one might have hoped that using experimentally derived geometries would have given a systematic error. The Xα approximation also omits any explicit correlation correction.[21] This term is about an order of magnitude smaller than the Xα exchange[31] although the use of an α value of 0.7 instead of the formal value of $\frac{2}{3}$ offsets this omission somewhat. Fortunately, the computed charge density appears relatively insensitive to these shortcomings and the DVXα scheme provides a quick method for surveying a range of molecules thereby identifying features worthy of more detailed examination. For quantitative accuracy, more sophisticated DFT methods are available.[32] Studies using these more advanced functionals are in progress.

Conclusion

In common with other studies in this laboratory,[2,10] the present DVXα calculations demonstrate that the bonding and reactivity of metal–dinitrogen complexes can be described by the static ground-state electron-density distributions. The computed overlap populations, atomic charges and frontier MO distributions correlate with the relative M–N_2 bond energies, N–N stretching frequencies, sites and relative rates of protonation and sites of attack by organic radicals. Even the non-relativistic treatment of $[W(PH_3)_4(N_2)_2]$ appears to give a reasonable charge distribution. However, attempts to obtain quantitative agreement *via* binding-energy calculations of bond energies and stretching frequencies gave relatively poor results.

Nevertheless, the qualitative success of these DVXα calculations is encouraging. In the light of recent advances in density functional theory,[31] the DVXα method must be viewed as relatively unsophisticated. However, it is a very fast scheme, even by DFT standards, and thereby offers an efficient way of obtaining reasonable results on a large number of molecules. We can then identify features worthy of more detailed examination by more sophisticated DFT methods.

Acknowledgements

The authors acknowledge the Science and Engineering Research Council Computational Science Initiative and the Royal Society for the provision of computer hardware.

References

1 B. E. Smith, in *Nitrogen Fixation. The Chemical-Biochemical-Genetic Interface*, eds. A. Muller and W. E. Newton, Plenum, New York, 1983, p. 23 and refs. therein; R. N. F. Thorneley and D. J. Lowe, in *Molybdenum Enzymes*, ed. T. G. Spiro, Wiley, New York, 1985, p. 221 and refs. therein; P. Pelikan and R. Boca, *Coord. Chem. Rev.*, 1984, **55**, 55.

2 J. J. R. Frausto da Silva and R. J. P. Williams, *The Biological Chemistry of the Elements: The Inorganic Chemistry of Life*, Oxford University Press, New York, 1991.

3 J. Chatt, J. R. Dilworth and R. L. Richards, *Chem. Rev.*, 1978, **78**, 589; F. A. Cotton and G. Wilkinson, *Advanced Inorganic Chemistry*, 5th edn., Wiley-Interscience, New York, 1988, p. 334 and refs. therein.

4 D. L. DuBois and R. Hoffmann, *Nouv. J. Chem.*, 1977, **1**, 479.

5 J. Kim and D. C. Rees, *Science*, 1992, **257**, 1677; J. Kim and D. C. Rees, *Nature*, 1992, **360**, 553.

6 H. B. Deng and R. Hoffmann, *Angew. Chem., Int. Ed. Engl.*, 1993, **32**, 1062.

7 P. Hohenberg and W. Kohn, *Phys. Rev. B*, 1964, **136**, 864; W. Kohn and L. J. Sham, *Phys. Rev. A*, 1965, **140**, 1133; W. Kohn and P. Vashishta, in *Theory of the Inhomogeneous Electron Gas*, eds. S. Lundqvist and N. H. March, Plenum, New York, 1983.

8 (*a*) T. Yoshida, T. Adachi, M. Kaminaka and T. Ueda, *J. Am. Chem. Soc.*, 1988, **110**, 4872; (*b*) T. Yoshida, T. Adachi, T. Ueda, M. Kaminaka, N. Sasaki, T. Higuchi, T. Aoshima, I. Mega, Y. Mizobe and M. Hidai, *Angew. Chem., Int. Ed. Engl.*, 1989, **28**, 1040.

9 D. E. Ellis and G. S. Painter, *Phys. Rev. B*, 1970, **2**, 2887; E. J. Baerends, D. E. Ellis and P. Ros, *Theor. Chim. Acta*, 1972, **27**, 339; E. J. Baerends, D. E. Ellis and P. Ros, *Chem. Phys.*, 1973, **2**, 41.

10 R. J. Deeth, *J. Chem. Soc. Dalton Trans.*, (*a*) 1990, 355; (*b*) 1990, 365; (*c*) 1991, 1467; (*d*) 1991, 1895.
11 F. W. Averill and D. E. Ellis, *J. Chem. Phys.*, 1973, **59**, 6412.
12 A. Rosen, D. E. Ellis, H. Adachi and F. W. Averill, *J. Chem. Phys.*, 1976, **65**, 3629.
13 R. S. Mulliken, *J. Chem. Phys.*, 1955, **23**, 1833, 1841.
14 E. J. Baerends, D. E. Ellis and P. Ros, *Theor. Chim. Acta*, 1972, **27**, 339.
15 T. Uchida, Y. Uchida, M. Hidai and T. Kodama, *Acta Crystallogr., Sect. B*, 1975, **31**, 1197.
16 S. N. Anderson, R. L. Richards and D. L. Hughes, *J. Chem. Soc., Dalton Trans.*, 1986, 245.
17 E. Carmona, J. M. Marin, M. L. Poveda, J. L. Atwood and R. D. Rogers, *Polyhedron*, 1983, **2**, 185.
18 R. A. Henderson, *J. Chem. Soc., Dalton Trans.*, 1984, 2259; W. Hussain, G. J. Leigh, H. M. Ali, C. J. Pickett and D. S. Rankin, *J. Chem. Soc., Dalton Trans.*, 1984, 1703.
19 J. E. Barclay, A. Hills, D. L. Hughes, G. J. Leigh, C. J. MacDonald, M. A. Bakar and H. M. Ali, *J. Chem. Soc., Dalton Trans.*, 1990, 2503.
20 B. Delley, D. E. Ellis, A. J. Freeman, E. J. Baerends and D. Post, *Chem. Rev. B*, 1983, **27**, 2132.
21 J. C. Slater, *Quantum Theory of Molecules and Solids*, McGraw-Hill, New York, 1974, vol. 4.
22 (*a*) S. Xiao, W. C. Trogler, D. E. Ellis and Z. Berkowitz-Yellin, *J. Am. Chem. Soc.*, 1983, **105**, 7033; (*b*) E. J. Baerends and P. Ros, *Chem. Phys.*, 1973, **2**, 52; (*c*) L. Fan, L. Versluis, T. Ziegler, E. J. Baerends and W. Ravenek, *Int. J. Quant. Chem., Quant. Chem. Symp.*, 1988, **22**, 173.
23 See A. Szabo and N. S. Ostlund, *Modern Quantum Chemistry: Introduction to Advanced Electronic Structure Theory*, Macmillan, New York, 1982, p. 196.
24 J. P. Maier and D. W. Turner, *J. Chem. Soc., Faraday Trans. 2*, 1972, 711.
25 D. W. Turner, C. Baker, A. D. Baker and C. Brundle, *Molecular Photoelectron Spectroscopy*, Wiley-Interscience, New York, 1970.
26 W. C. Trogler, D. E. Ellis and J. Berkowitz, *J. Am. Chem. Soc.*, 1979, **101**, 5896; B. E. Bursten, M. Casarin, D. E. Ellis, I. Fragala and T. J. Marks, *Inorg. Chem.*, 1986, **25**, 1257; M. Sano, H. Adachi and H. Yamatera, *Bull. Chem. Soc. Jpn.*, 1982, **55**, 1022.
27 J. N. Murrell, A. Al-Derzi, G. J. Leigh and M. F. Guest, *J. Chem. Soc., Dalton Trans.*, 1980, 1425.
28 M. A. Buijse and E. J. Baerends, *J. Chem. Phys.*, 1990, **93**, 4129.
29 P. Brant and R. D. Feltham, in *Proceedings of the 2nd Climax International Conference on the Chemistry of Molybdenum*, Oxford, 1976.
30 J. Chatt, W. Hussain, G. J. Leigh, H. Neukomm, C. J. Pickett and D. Rankin, *J. Chem. Soc., Chem. Commun.*, 1980, 1024.
31 T. Ziegler, *Chem. Rev.*, 1991, **91**, 651.
32 R. J. Deeth, *J. Chem. Soc., Dalton Trans.*, 1993, 1061; *J. Phys. Chem.*, 1993, **97**, 11625; *J. Chem. Soc., Faraday Trans.*, 1993 3745; C. Sosa, J. Andzelm, B. C. Elkin, E. Wimmer, K. D. Dobbs and D. A. Dixon, *J. Phys. Chem.*, 1992, **96**, 6630.

Received 15*th November* 1993; *Paper* 3/06806D